

1 **The *Plasmodium falciparum* CCCH zinc finger protein ZNF4**

2 **plays an important role in gametocyte exflagellation**

3 **through the regulation of male gametocyte enriched**

4 **transcripts**

5 Short title: ZNF4 is vital for gametocyte exflagellation.

6
7 Borja Hanhsen, Afia Farrukh, Gabriele Pradel and Che Julius Ngwa*

8
9 Division of Cellular and Applied Infection Biology, Institute of Zoology, RWTH Aachen
10 University, Aachen, Germany

11
12
13
14

15 *corresponding author:

16 ngwa.che@bio2.rwth-aachen.de

17
18
19
20
21
22
23
24
25
26
27
28
29
30
31
32
33
34

35 Abstract

36
37 CCCH zinc finger proteins (ZFPs) function mainly as RNA-binding proteins (RBPs) where they
38 play a central role in the mRNA metabolism. Over 27 CCCH-ZFPs are encoded in the genome
39 of the human malaria parasite *Plasmodium falciparum*, the causative agent of malaria tropica.
40 However, little is known about their functions. In this study, we characterize one member of
41 the PfCCCH-ZFP named ZNF4. We show that ZNF4 is highly expressed in mature gametocytes
42 where it predominantly localizes to the cytoplasm. Targeted gene disruption of ZNF4 showed
43 no significant effect in asexual blood stage replication and gametocyte development while
44 male gametocyte exflagellation was significantly impaired leading to reduced malaria
45 transmission in the mosquito. Comparative transcriptomics between wildtype (WT) and the
46 ZNF4-deficient line (ZNF4-KO) demonstrated the de-regulation of about 473 genes (274-
47 upregulated and 199 down-regulated) in mature gametocytes. Most of the down-regulated
48 genes show peak expression in mature gametocyte with male enriched genes associated to
49 the axonemal dynein complex formation and cell projection organization highly affected,
50 pointing to the phenotype in male gametocyte exflagellation. Up-regulated genes are
51 associated to ATP synthesis. Our combine data therefore indicate that ZNF4 is a CCCH zinc
52 finger protein which plays an important role in male gametocyte exflagellation through the
53 regulation of male gametocyte enriched genes.

54 Author Summary

55
56 CCCH ZFPs have gained significant interest due to their ability to interact with RNA and control
57 different RNA metabolic processes. The role of CCCH ZFPs in the malaria parasite *Plasmodium*
58 *falciparum* has not been well studied. In this study we report the functional characterization
59 of a PfCCCH-ZFP named ZNF4. Using mouse anti-ZNF4 antisera and a ZNF4-HA tag parasite line

60 we show that the protein is mainly expressed in the cytosol of mature gametocytes. To
61 determine the function of ZNF4, we generated a ZNF4 knockout parasite line and we found
62 that the asexual blood stages and gametocytes developed normally while the ability of the
63 male gametocytes to exflagellate as well as the further development of the parasite in the
64 mosquito was significantly impaired. Interestingly, when the transcriptome of mature
65 gametocytes of the ZNF4-KO was compared to the WT, down-regulated genes were mainly
66 male gametocyte enriched genes associated to processes involved in gametocyte
67 exflagellation such axonemal dynein complex formation and cell projection organization
68 indicating that ZNF4 plays an important role in male gametocyte exflagellation through the
69 regulation of male gametocyte enriched transcripts.

70 Introduction

71

72 Malaria is one of the deadliest parasitic diseases which resulted in over 241 million infections
73 and 627 000 deaths in 2020 [1]. The disease is caused by apicomplexan parasites of the genus
74 *Plasmodium* with *P. falciparum* as the caustic agent of malaria tropica causing the most severe
75 form. Malaria is transmitted from the human to the anopheline mosquito by a subset of
76 specialized cells, the gametocytes which leave the asexual replication cycle and differentiate
77 into male and female forms. Once mature, the gametocytes are picked up by a blood feeding
78 mosquito. In the midgut of the mosquito, they become activated by external stimuli then the
79 male gametocytes undergo exflagellation, a process that includes three rounds of DNA
80 replication followed by the release of 8 motile microgametes, while the females develop into
81 macrogametes. Following fusion of a microgamete and a macrogamete, a zygote forms during
82 the first hour post-activation, which transforms into an infective ookinete within the following

83 24 h. The motile ookinete traverses the midgut epithelium before settling down and forming
84 an oocyst between epithelium and basal lamina [2,3].
85 Gametocyte development as well activation in the mosquito midgut is supported by a well-
86 coordinated sequences of gene activation and silencing events, which are essential to prepare
87 the parasite for transmission from the human to the insect host. Research over the past
88 decade has demonstrated a pivotal role of transcriptional and translational regulation in this
89 process. Gametocyte commitment, the process by which asexual blood stage parasites enter
90 the sexual pathway to form gametocytes, has been shown to be regulated by the transcription
91 factor AP2-G. The expression of AP2-G promotes the transcription of early gametocyte genes,
92 which leads to gametocyte commitment and formation [4–6]. In a recent study, it was shown
93 that another transcription factor AP2-G5 is essential for gametocyte maturation through the
94 down-regulation of AP2-G and a set of genes activated by AP2-G prior to gametocyte
95 development [7]. Other transcription factors such as AP2-FG and AP2-O3 have been shown to
96 regulate gene expression in female gametocytes [8,9] and ookinete development by AP2-O
97 family [10,11].
98 An important mechanism of transcript regulation is translational repression which has been
99 shown to play an important role in the regulation of female gametocyte transcripts of the
100 malaria parasite. Transcripts of parasite required for mosquito midgut stage formation is
101 synthesized and stored in granules in female gametocytes, where they are translationally
102 repressed by binding to regulatory ribonucleoprotein complexes and the repression is only
103 released after gametocyte activation to promote zygote to ookinete formation [12,13]. In *P.*
104 *berghei*, the RNA helicase DOZI (development of zygote inhibited) and the Sm-like factor CITH
105 (homolog of worm CAR-I and fly Trailer Hitch) play central roles in the formation of the
106 ribonucleoprotein complex which stores several transcripts including P25 and P28 which are

107 later released after gametocyte activation for zygote to ookinete development [14,15]. In *P.*
108 *falciparum* on the other hand, the Pumilio/Fem-3 binding factor (Puf) family Puf2 which is an
109 RBP together with its interaction partner 7-helix-1 have been shown to be involved in
110 translational repression of a number of gametocyte transcripts including Pfs25 and Pfs28
111 [13,16]. Also, the RBP Puf1 has been shown to play an important role in the differentiation and
112 maintenance of mainly female gametocytes [17].
113 To date, little is known how the transcripts are regulated in male gametocytes. In previous
114 studies, we carried out chemical loss of function studies using inhibitors targeting histone
115 modification enzymes and we showed significant de-regulation of genes expression in
116 immature, mature and activated gametocytes following treatment with the inhibitors [18,19].
117 These studies indicated epigenetic gene regulation mechanisms during gametocyte
118 development and potentially in male and female gametocytes. In one of the study, we
119 identified a CCCH-ZFP which we named ZNF4 (PF3D7_1134600) that was highly de-regulated
120 following the treatment of the immature gametocytes with the histone deacetylase inhibitor
121 Trichostatin A [18]. CCCH-type zinc finger proteins mainly act as RBP with important roles in
122 the RNA metabolism including RNA stability and transcriptional repression [20,21]. In some
123 cases, CCCH-ZFPs may traffic between the nucleus and the cytoplasm [22] and bind both DNA
124 and RNA [23], thereby functioning in both DNA and RNA regulation [24]. We now show that
125 ZNF4 is a potential nucleic acid-binding protein which plays an important role in microgamete
126 exflagellation through the regulation of male-specific genes during gametocyte development.
127
128
129

130 **Results**

131

132 **ZNF4 is a CCCH-ZFP expressed mainly in gametocytes of *P. falciparum***

133

134 Analysis of the ZNF4 protein features using UniProt shows a 204 kDa protein with three CCCH

135 zinc finger domains between amino acid 513 to 540, 548 to 574 and 582 to 610 (Fig 1A). In

136 addition, the 3D-structure of the protein as predicted using AlphaFold [25,26] shows the

137 arrangement of alpha helices and the beta strands in the CCCH domains to coordinate the zinc

138 binding (Fig 1B). To determine the transcript expression of ZNF4, a semi quantitative RT-PCR

139 was performed using asexual blood stages (rings, trophozoites and schizonts) as well as

140 gametocyte stages (immature, mature and 30 min post-activated gametocytes). The

141 transcript levels of Pfama1 (apical membrane antigen 1) and Pfccp2 (LCCL domain-containing

142 protein) were determined to control for purity in asexual blood stage and gametocyte samples

143 respectively. Samples without reverse transcriptase (-RT) were used as controls to verify the

144 absence of genomic DNA. Pffbp1 (fructose-bisphosphate aldolase) was used as housekeeping

145 loading control. High transcript expression of ZNF4 was observed in the gametocyte stages as

146 compared to the asexual blood stages (Fig 1C). To determine the ZNF4 protein expression, a

147 recombinant peptide (RP) corresponding to a portion of ZNF4 (Fig 1A) was expressed in *E. coli*

148 and used to generate mouse polyclonal antisera against ZNF4. Immunofluorescence assays

149 (IFAs) show mainly a cytoplasmic expression of ZNF4 in both asexual blood stages and

150 gametocytes with the highest expression in mature gametocytes (Fig 1D). Differences in sex

151 specific expression between male and female gametocytes were not observed. To confirm

152 ZNF4 expression, we used a pSLI-ZNF4-HA-glmS parasite line in which the 3'end of the

153 endogenous gene was fused with the sequence of a 3x HA-tag and a glmS ribozyme (Fig S1A).

154 Successful integration in the parasite line was obtained (Fig S1B) and we were able to detect

155 the HA-tagged ZNF4 in mature gametocyte lysates at a molecular weight of roughly 250 kDa
156 (Fig S1C). IFAs using anti-HA confirmed expression of the protein in the asexual blood stages
157 and gametocytes with the highest expression in mature gametocytes (Fig S1D).

158 **Targeted gene disruption of ZNF4 does not impact asexual blood stage**
159 **replication and gametocyte development**

160 To determine the function of ZNF4, we utilized the selected linked integration-mediated
161 targeted gene disruption method [27] to generate a disrupted ZNF4 parasite line, named
162 ZNF4-KO (Fig 2A). These parasites express only a truncated N-terminal GFP tagged fragment
163 which lacks the three CCCH zinc finger domains. Successful disruption was confirmed by
164 diagnostic PCR, which indicated 5' and 3' integration and lack of wildtype in the ZNF4-KO
165 parasite line (Fig 2B). To further confirm the gene disruption, the remaining part of the ZNF4-
166 KO truncated protein which is fused to GFP was detected by Western Blotting using different
167 parasite stages (rings, trophozoites, schizonts, immature and mature gametocytes) as well as
168 by live imaging (Fig 2C, D). The western blotting with the ZNF4-KO parasite line further
169 confirmed the expression of the truncated protein at the expected molecular weight of 53 kDa
170 in different *P. falciparum* stages (Fig 2C).

172 After successful gene disruption, we first examined the asexual blood stage replication in the
173 ZNF4-KO line. To this end, the development of highly synchronized ring stages of the ZNF4-KO
174 and WT parasite lines was monitored over a period of 96 h by Giemsa stained blood smears,
175 which were taken every 12 h. The results show no significant difference in intraerythrocytic
176 replication between the ZNF4-KO and the WT (Fig 2E). Then rings stage parasites after the
177 second replication cycle were induced for gametocytogenesis and asexual blood stages were
178 eliminated. Gametocyte development and gametocytaemia were followed from day 5 post-
179 activation till day 10. No significant effect in gametocytaemia and gametocyte development

180 was observed (Fig 2F, G). In addition, the morphology of ZNF4-KO gametocytes was not
181 affected (Fig 2H).

182 **Disruption of ZNF4 impacts microgamete exflagellation and reduces
183 transmission in the mosquito**

184
185 To determine if male gametocytes of the ZNF4-KO parasite line are able to produce motile
186 microgametes, an *in vitro* exflagellation assay was performed. To this end, mature
187 gametocytes of the ZNF4-KO and WT were activated with xanthurenic acid (XA) for 15 min at
188 RT. After activation, the numbers of exflagellation centres were counted microscopically. The
189 results show that the ZNF4-KO produced significantly lower numbers of exflagellation centres
190 as compared to WT (Fig 3A) indicating an impairment in male gametocyte exflagellation. To
191 see if this impairment can affect malaria transmission in the mosquitoes, the matured
192 gametocytes were fed to *Anopheles stephensi* mosquito in membrane feeding assays and the
193 number of oocysts were counted. Although the ZNF4-KO line still produced oocysts, their
194 numbers were relatively very low as compared to the WT (Fig 3B).

195 **ZNF4 disruption results in down-regulation of male gametocyte
196 enriched transcripts.**

197
198 To compare the transcriptome of the ZNF4-KO and the WT, we carried out a comparative RNA-
199 Seq using ring stage parasites and mature gametocytes of the ZNF4-KO and the WT. We used
200 a cut off of greater than 2-fold change in expression. The results show that 66 genes were de-
201 regulated in the ring stage following ZNF4 disruption (55 down-regulated and 11 up-regulated)
202 as opposed to mature gametocytes to which a total of 473 genes (274 up-regulated and 199
203 down-regulated) were detected (Fig 4A, Table S1). For further analysis, we then focused on
204 the de-regulated genes in mature gametocytes, since the knockout phenotype suggests that
205 male gametocyte exflagellation was affected. To validate the RNA-Seq data, we carried out a

206 quantitative real-time experiment (qRT) to compare the transcript expression of 8 genes (5
207 up-regulated and 3 down-regulated) using RNA from mature gametocytes of the ZNF4-KO and
208 the WT. The results confirmed the RNA-Seq data as four of the five up-regulated genes in the
209 RNA-Seq data were up-regulated and all down-regulated genes were down-regulated in the
210 qRT (Fig 4B).

211 We next performed a gene ontology (GO) enrichment analysis (Table S1). Down-regulated
212 genes could mainly be assigned to biological processes such as regulation of microtubule-
213 based processes, cell projection organization and cilium organization (Fig 4C). Regarding
214 cellular components, axonemal dynein complex assembly was highly represented and for
215 molecular function, dynein light chain binding and microtubule binding was also highly
216 represented (Fig 4C). Up-regulated genes were mainly assigned to nucleoside containing small
217 molecule metabolic processes and the respiratory electron transfer chain as biological
218 processes. In addition, the respiratory chain complex, the mitochondrial respiratory chain
219 complex (cellular component) as well as electron transfer activity and oxidoreductase activity
220 (molecular function) were the mostly represented (Fig 4D).

221 We also determined at which stage of the parasite life cycle does the de-regulated genes show
222 peak expression according to the seven stage RNA-Seq data [28]. We observed that most of
223 the down-regulated genes show peak expression in stage V gametocytes followed by the
224 ookinete stage (Fig 4E). On the other hand, the up-regulated genes showed peak expression
225 in stage II and stage V gametocytes (Fig 4E).

226 Since the disruption of ZNF4 mainly affected male gametocyte exflagellation, we analyzed if
227 the effect was due to the down-regulation of transcripts enriched in male gametocytes. For
228 this reason, we compared the sex specific transcript expression of the top 30 down-regulated
229 genes using the sex specificity data from Lassonder and colleagues [29]. The heat map shows

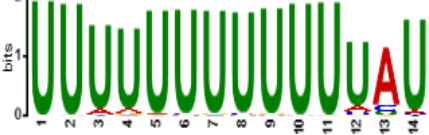
230 that indeed most of the down-regulated genes have high transcript levels in male gametocytes
231 with genes like PF3D7_1469900 (male gametocytes enriched transcribe, MGET) and
232 PF3D7_1311100 (meiosis-specific nuclear structural protein 1, putative) present (Fig 4F).

233
234 **ZNF4-KO up-regulated and down-regulated genes show different**
235 **predicted enriched RNA binding motifs.**

236
237 To determine the predicted RNA-binding motif in the de-regulated mature gametocyte genes,
238 the comprehensive motif analysis tool XSTREME (Meme-suite.org; [31]) was used to check
239 which motifs were enriched in the up-regulated and down-regulated genes as compared to
240 the control transcripts which were not affected. We used downloaded transcript sequences
241 from the PlasmoDB website (plasmodb.org/plasmo/app) containing the 5' and 3'UTR and
242 search for motif of 7 to 15 nucleotides. In the up-regulated genes motifs identified were U-
243 rich with the top two hits being "UUUUUUUUUUUUUAU" with this signature found in 199 of
244 the 274 up-regulated transcripts (e-value: 1.8e-015; Table 1) and "AUUUUUAUUUU" with this
245 signature found in 207 of the 274 genes (e-value: 1.5e-010; Table 1). On the other hand, motifs
246 of the down-regulated genes were mainly A-rich with top hits being "AAAAUAUAAAAAAA"
247 with this signature in 138 of the 199 down-regulated genes (e-value: 3.3e-012; Table 1) and
248 "AAAAAAAAGAAAA" with signature in 165 out of the 199 down-regulated genes and (e-value:
249 5.8e-011; Table 1). Interestingly, these motifs were highly similar to known RBP motifs (Table
250 1). This indicates that ZNF4 is probably binding to different motifs in the up-regulated and
251 down-regulated genes.

252
253
254
255
256

257 Table 1: Predicted binding motif for ZNF4-KO in the up-regulated and down-regulated genes.

ZNF4-KO	Predicted motif	No of positive genes (%)	E-value	Similar known motif [32]
Up-regulated genes		199 (72.6%)	1.8e-015	SXL (RNCMPT00119) Pp_0228 (RNCMPT00228) Tv_0236 (RNCMPT00236)
		207 (75.5 %)	1.5e-010	HuR (RNCMPT00032) HNRNPC (RNCMPT00025) HNRNPL1 (RNCMPT00167)
Down-regulated genes		138 (69.3%)	3.29e-012	KHDRBS1 (RNCMPT00169) Lm_0255 (RNCMPT00255) PABPC4 (RNCMPT00043)
		165 (82.9%)	5.82e-011	Nab2p (RNCMPT00042) Hnrnpr (RNCMPT00289) PABPC4 (RNCMPT00043)

258

259 Discussion

260
261 The highly complex life cycle of the human malaria parasite *P. falciparum* requires a well-
262 coordinated gene regulation to allow for gametocyte commitment, development and human
263 to mosquito transmission of the parasite. Translational repression in particular has been
264 shown to be the main player in preparing female gametocytes for parasite transmission with
265 RNA-binding translational repressors like DOZI, CITH or Puf2 playing crucial roles. While the
266 mechanism by which female gametocytes genes are regulated has been studied in detail, the
267 mechanism of regulation of male-specific genes remains largely unknown. In the present study,
268 we show that the PfCCCH ZFP named ZNF4 is a potential RBP important for male
269 gametogenesis and hence malaria transmission through the regulation of male-enriched
270 gametocyte genes. Noteworthy, ZNF4 is expressed mainly in the cytoplasm of both male and

271 female gametocytes in accord with previous sex- specificity data [29], indicating that ZNF4
272 expression is not dependent of the gametocyte sex of the parasite.

273 Targeted gene disruption of *ZNF4* showed normal progression through the intraerythrocytic
274 replication cycle indicating that the gene is dispensable for asexual blood stage replication.

275 This is not surprising as a recent genome-wide transposon mutagenesis screen in *P. falciparum*
276 also indicates that the gene is not essential for parasite viability [33]. Also, the ZNF4-KO
277 parasite line did not show any significant effect in gametocyte formation and development
278 with the gametocytes showing normal morphology. However, although gametocyte
279 development was not affected, *ZNF4* disruption greatly impaired malaria transmission in the
280 mosquito through the inhibition of exflagellation and in consequence oocyst formation. A
281 recent study also linked the involvement a *P. berghei* RNA binding protein UIS12 to
282 gametocyte exflagellation and malaria transmission [34].

283 To determine the possible cause on exflagellation inhibition in the ZNF4-KO, we carried out
284 comparative transcriptomic analysis in mature gametocytes as well as ring stages. Only a few
285 genes (64) were > 2-fold de-regulated in the ring stage following *ZNF4* disruption which is in
286 accord with the lack of any phenotype during asexual blood stage replication indicating that
287 *ZNF4* has no special role in ring stage parasites. 427 genes were de-regulated in ZNF4-KO
288 mature gametocytes (274 genes up-regulated and 199 down-regulated), pointing to the effect
289 in male gametocyte exflagellation.

290 Further analysis demonstrated that the majority of the down-regulated genes exhibit peak
291 expression in mature gametocytes where they are implicated in essential cellular and
292 biological processes linked to male gametogenesis such as cell projection assembly, cilium
293 assembly and the axonemal dynein complex. The up-regulated genes mainly exhibit peak
294 expression in stage II gametocytes with represented cellular and biological processes

295 associated to the respiratory electron chain and mitochondrial ATP synthesis. Interestingly, a
296 previous study which integrated transcriptomics and proteomic, associated male gametocytes
297 to be enriched in proteins associated to formation of flagellated gametes, axoneme formation,
298 DNA replication and chromatin organization while female gametocytes were enriched with
299 proteins associated to protein, lipid and energy metabolism [29]. The down-regulation of
300 genes mainly associated to cell projection assembly, cilium assembly and axonemal dynein
301 complex formation therefore justifies the defect in male gametocyte exflagellation and
302 studies in other organisms have associated the processes to proper flagella formation,
303 movement and fertility [35,36]. Regarding the up-regulated genes following ZNF4-KO, it is
304 likely that since energy metabolism is not very necessary for male gametocytes, these genes
305 are being repressed in male gametocytes by ZNF4 and they become up-regulated following
306 ZNF4 disruption. In accord with our findings, the top 30 down-regulated genes showed high
307 expression in male gametocytes. Although the function of most of the male highly expressed
308 genes are unknown, some prominent genes encode for PF3D7_1469900 (PfMGET), an
309 abundant protein transcribed specifically in male gametocytes which has been used for male
310 gametocyte quantification [37,38] and for PF3D7_1311100 (meiosis-specific nuclear
311 structural protein 1, putative) with human homolog MSN1 which has been linked to male
312 fertility [39,40].

313 An interesting finding in this study is the fact that up-regulated genes and down-regulated
314 genes possess different binding motifs suggesting that they may be regulated differently. The
315 motifs for the up-regulated genes have been reported to bind RBPs such as SXL and HuR. SXL
316 also known as sex lethal is a master regulator of sex determinant in *Drosophila melanogaster*
317 by regulating the choice between male and female development pathways [41,42]. For the
318 down-regulated gene motifs, they have been reported as targets for RBPs like Nab2p and

319 PABC4. Nabp2 in *Saccharomyces cerevisiae* is a nuclear protein required to protect early
320 mRNA and has also been reported to be involved in RNA export from the nucleus to the
321 cytoplasm [43,44]. PABC4 (cytoplasmic poly(A) binding protein C4) exhibit a critical role in
322 erythroid differentiation through mRNA regulation [45].
323 The exact mechanism by which ZNF4 regulates gene expression warrants further investigation.
324 One potential mechanism could be by translational repression as has been shown for female
325 gametocytes where mRNA transcripts important for zygote/ookinete development such as
326 P25 and P28 are stored in a messenger ribonucleoprotein complex composed of RNA binding
327 protein like DOZI and CITH in *P. berghei* [14,15] or Puf2 and 7-Helix-1 in *P. falciparum* [13,46].
328 Noteworthy, a recent study in *P. berghei* has identified a CCCH domain containing ZFP, Pb103
329 to be associated to zygote/ookinete development probably by translational repression [47]. It
330 is likely that there exists a translational repression mechanism regulating male gametocyte
331 genes in which ZNF4 is part of the complex.
332 Another probable mechanism by which ZNF4 controls transcripts is by the regulation of mRNA
333 stability as has been reported for many CCCH-ZFPs such as the tristetraprolins (TTPs) which
334 are the most studied CCCH-ZFPs. TTPs have been shown to bind AU-rich elements in mRNAs,
335 resulting in the removal of the poly-A tail from the mRNA, thereby marking them for decay
336 [48]. It is possible that the deficiency of ZNF4 leads to the accumulation of transcripts due to
337 the absence of mRNA stabilization as observed with the up-regulated genes.
338 In conclusion, we have identified a novel ZFP, ZNF4 and demonstrated that ZNF4 plays an
339 essential role in the regulation of male gametocyte genes which are important of
340 microgamete exflagellation, fertilization and parasite transmission in the mosquito. However,
341 further studies will be required to address the mechanism by which ZNF4 regulates the gene
342 expression and if more critical regulatory proteins are involved.

343 **Materials and Methods**

344

345 **Antibodies**

346

347 Antibodies used in this study included: rabbit anti-HA (Sigma Aldrich, Taufkirchen, Germany),

348 rat anti-HA (Roche, Basel, Switzerland), mouse anti-GFP (Roche, Basel, Switzerland),

349 mouse/rabbit anti-Pfs230 [49], rabbit/mouse anti-Pf39. Mouse anti-ZNF4 was generated for

350 this study (see below). For indirect immunofluorescence assays (IFAs), the following dilutions

351 of the antibodies were used: mouse/rabbit anti-Pfs230 (1:200), mouse anti-ZNF4 (1:20),

352 mouse anti GFP (1:200), rabbit anti HA (1:50). For Western blot analysis the following dilutions

353 were used: rat/rabbit anti-HA (1:500), rabbit anti-Pf39 (1:10000), anti-GFP (1:1000).

354 **Parasite culture**

355

356 The *P. falciparum* gametocyte-producing strain NF54 was used as background strain in this

357 study. The parasites were cultivated *in vitro* in RPMI 1640/HEPES medium (Gibco, Thermo

358 Scientific Waltham, USA) supplemented with 10% heat-inactivated human serum and A⁺

359 erythrocytes at 5% hematocrit as described [50]. As supplement, 50 µg/ml hypoxanthine

360 (Sigma Aldrich, Taufkirchen, Germany) and 10 µg/ml gentamicin (Gibco, Thermo Scientific

361 Waltham, USA) were added to the cell culture medium and the cultures were grown in an

362 atmosphere of 5% O₂, 5% CO₂, 90% N₂ at a constant temperature of 37°C. Cultures were

363 synchronized by repeated sorbitol treatment as described [51].

364 Human erythrocyte concentrate and serum were purchased from the Department of

365 Transfusion Medicine (University Hospital Aachen, Germany). The University Hospital Aachen

366 Ethics commission approved all work with human blood, the donors remained anonymous

367 and serum samples were pooled.

368

369 **Generation of mouse antisera**

370

371 A recombinant protein, corresponding to a portion of ZNF4 (Fig 1A), was expressed as maltose-
372 binding protein-tagged fusion protein using the pMAL™c5X-vector (New England Biolabs,
373 Ipswich, USA). The coding DNA sequence was amplified by PCR using gene-specific primers
374 (for primer sequences, see Table S2). Recombinant protein was expressed in *E. coli* BL21 (DE3)
375 RIL cells according to the manufacturer's protocol (Invitrogen, Karlsruhe, Germany) and
376 isolated and affinity-purified using amylose resin according to the manufacturer's protocol
377 (New England Biolabs, Ipswich, USA). Polyclonal antisera were generated by immunization of
378 6-weeks old female NMRI mice (Charles River Laboratories, Wilmington, USA) subcutaneously
379 with 100 µg recombinant protein emulsified in Freund's incomplete adjuvant (Sigma Aldrich,
380 Taufkirchen, Germany) followed by a boost after 4 weeks. At day 10 after the boost, mice
381 were anesthetized by intraperitoneal injection of a mixture of ketamine and xylazine
382 according to the manufacturer's protocol (Sigma Aldrich, Taufkirchen, Germany), and immune
383 sera were collected via heart puncture. The immune sera of three mice immunized were
384 pooled; sera of three non-immunized mice (NMS) were used as negative control. Experiments
385 in mice were approved by the animal welfare committee of the District Council of Cologne,
386 Germany (ref. no. 84-02.05.30.12.097 TVA).

387 **Generation of ZNF4-KO parasite line**

388

389 Disruption of ZNF4 (PF3D7_1134600) was achieved by selection-linked integration as
390 described [27]. Briefly, the plasmid pSLI-TGD-GFP was modified to contain a 601 bp homology
391 block from the 5' end of the ZNF4 coding region (for primer sequence see Table S2). Parasites
392 were transfected as described [18] and WR99210 (Jacobus Pharmaceuticals, New Jersey, USA)
393 was added to a final concentration of 4 nM, starting at 6 h after transfection to select
394 integrated parasites. WR99210-resistant parasites appeared after 21 days and they were

395 treated with medium containing 400 µg/ml G418 (Sigma Aldrich, Taufkirchen, Germany) and
396 correct integration confirmed by diagnostic PCR (for primer sequences, see Table S2). After
397 successful integration was obtained, the lines were maintained through selection with 4 nM
398 WR99210.

399 **Generation of ZNF4-HA-glmS parasite lines**

400
401 To generate a ZNF4-HA-glmS parasite line, we used selected linked integration insertion using
402 a pSLI-HA-glmS vector (kindly provided by Dr. Ron Dzokowski, the Hebrew University of
403 Jerusalem) in which the plasmid was modified to contain a homology block from the 3' end of
404 the *ZNF4* gene excluding the stop codon (for primer sequence see Table S2). Parasites were
405 transfected and WR99210 was added to a final concentration of 4 nM, starting at 6 h after
406 transfection to select integrated parasites. WR99210-resistant parasites appeared after 21
407 days and they were treated with medium containing 400 µg/ml G418 and correct integration
408 confirmed by diagnostic PCR (for primer sequences, see Table S2).

409 **RNA isolation and RNA sequencing**

410
411 Total RNA was isolated from ring stage and Percoll- enriched mature (stage V) gametocytes
412 from the ZNF4-KO and NF54 WT using the Trizol reagent (Invitrogen, Karlsruhe, Germany)
413 according to the manufacturer's protocol. Quality of RNA samples were assessed using a ND-
414 1000 (NanoDrop Technologies, Thermo Scientific Waltham, USA) and by agarose gel
415 electrophoresis.

416 RNA sequencing was performed at the Genomic Facility of the University Clinic at the RWTH
417 University Aachen, Germany. Briefly, the quality of the isolated total RNA samples from ring
418 stage and mature gametocytes of the ZNF4-KO and the WT were evaluated by Tapestation
419 4200 (Agilent Technologies, Santa Clara, USA). The quantities were measured by Quantus
420 Fluorometer (Promega, Manheim, Germany). Libraries were generated with TruSeq Stranded

421 mRNA Library Preparation kit (Illumina) from high quality total RNA samples according to the
422 manufacturer's protocol. The generated libraries, which pass the QC check on Tapestation
423 4200 (Agilent Technologies, Santa Clara, USA) were sequenced on a NextSeq 500 (Illumina)
424 with High output Kit v2.5 (150 cycles) for paired-end sequencing according to standard
425 procedure provided by Illumina.

426 Data were analyzed with the NextGen pipeline, an in house-adapted pipeline embedded in
427 the workflow management system of the QuickNGS-Environment [52]. In detail, the data
428 were first demultiplexed according to corresponding indices. After quality assessment of the
429 resulted fastq files with FastQC (v0.11.5), STAR v2.5.2b [53] was applied to align the reads to
430 the *P. falciparum* 3D7 EPr1 (version 43) with default parameters. Aligned reads were
431 quantified with Stringtie v1.3.6 as described [54]. Counts for transcripts were counted with
432 featureCounts subread v 1.5.1 [55] and differential expression analysis were finally conducted
433 by comparing the transcript levels in the RNA samples of the ZNF4-KO and wildtype parasites
434 for each stage using DESeq2 -R version 3.5.1 [55]. Raw data have been submitted to the NCBI
435 Gene Expression Omnibus (GEO; <http://www.ncbi.nlm.nih.gov/geo/>) under accession number
436 GSE196298.

437 **Semi- quantitative RT-PCR**

438
439 To determine the transcript expression of ZNF4, total RNA was isolated from rings,
440 trophozoites, schizonts, immature, mature and 30 min post-activated gametocytes as
441 described above. One µg of each RNA sample was used for cDNA synthesis using the
442 SuperScript IV First-Strand Synthesis System (Invitrogen, Karlsruhe, Germany), following the
443 manufacturer's instructions. The synthesized cDNA was first tested by diagnostic PCR for
444 asexual blood stage contamination using specific primers and controls without reverse
445 transcriptase were also used to investigate potential gDNA contamination [19]. Transcript for

446 ZNF4 (250 bp) was amplified using ZNF4 RT primers (for primer sequences, see Table S1). The
447 following condition was used, Initial denaturation at 94°C for 2 min, followed by 25 cycles of
448 denaturation at 94°C for 30 s, of annealing at 45°C for 30 s, and of elongation at 72°C for 30 s,
449 and a final extension at 72°C for 2 min.

450 Real-time RT-PCR

451
452 To validate the RNA -Seq data, 1 µg of total RNA from mature gametocytes from the ZNF4-KO
453 and WT parasite line was used for cDNA synthesis using the SuperScript IV First-Strand
454 Synthesis System following the manufacturer's instructions (Invitrogen, Karlsruhe, Germany).
455 The synthesized cDNA was first verified by diagnostic PCR for asexual blood stage and DNA
456 contamination using specific primers as described [18,19]. Primers for qRT-PCR corresponding
457 to eight up-regulated and three down-regulated genes in the ZNF4-KO were designed using
458 the Primer 3 software (<http://frodo.wi.mit.edu/primer3/>) and tested in conventional PCR
459 using DNA or cDNA to confirm primer specificity (for primer sequences, see Table S2). Real-
460 time RT-PCR measurements were performed using the Step One Plus Real-Time Detection
461 System (Thermo Scientific, Waltham, USA). Reactions were performed in triplicate in a total
462 volume of 20 µl using the maxima SyBR green qPCR master mix according to manufacturer's
463 instructions (Thermo Scientific, Waltham, USA). Controls without template and without
464 reverse transcriptase were included in all qRT-PCR experiments. The levels of transcript
465 expression were calculated by the $2^{-\Delta Ct}$ method [56] using the endogenous control gene
466 encoding the *P. falciparum* seryl tRNA-ligase (PF3D7_0717700) as reference [57,58].

467 Western blotting

468
469 Asexual blood stage parasites of the WT or mutant parasite lines were obtained following
470 tightly synchronization of cultures with 5% sorbitol [51], while gametocytes were enriched by
471 Percoll gradient purification [59]. Parasites were released from iRBCs with 0.05% w/v

472 saponin/PBS for 10 min at 4°C, washed with PBS and resuspended in lysis buffer (0.5% Triton
473 X-100, 4% w/v SDS, 0.5xPBS) supplemented with protease inhibitor cocktail (Roche, Basel,
474 Switzerland). The lysates were then resuspended in 5 x SDS-PAGE loading buffer containing
475 25mM DTT, heat-denatured for 10 min at 95°C, and then separated via SDS-PAGE. After the
476 protein have been separated, they were then transferred to Hybond ECL nitrocellulose
477 membrane (Amersham Biosciences) according to the manufacturer's protocol. Membranes
478 were blocked for non-specific binding by incubation in Tris-buffered saline containing 5%
479 skimmed milk and 1% BSA, followed by incubation with the respective primary antibody at
480 4°C overnight. After washing, the membranes were incubated with an alkaline phosphatase-
481 conjugated secondary antibody directed against the first antibody (Sigma Aldrich, Taufkirchen,
482 Germany) for 1 h at RT and developed in a solution of nitroblue tetrazolium chloride (NBT)
483 and 5-bromo-4-chloro-3-indoxyl phosphate (BCIP; Sigma Aldrich, Taufkirchen, Germany) for
484 5-30 min.

485 **Indirect immunofluorescence assay**

486
487 Mixed cultures of the WT or mutant parasite lines were air-dried on glass slides and fixed for
488 10 min in a methanol bath at -80°C. The RBCs were membrane permeabilized to allow access
489 to the parasites and non-specific binding sites were blocked by incubating the fixed cells in
490 0.01% saponin/0.5% BSA/PBS and 1% neutral serum each for 30 min at RT. Afterwards, the
491 preparation was then incubated with the primary antibody diluted in 0.01% saponin/0.5%
492 BSA/PBS for 2 h each at 37°C. Binding of primary antibody was visualized by incubating the
493 preparations with Alexa Fluor 488-conjugated secondary antibody directed against the
494 primary antibody (Thermo Fisher Scientific, Waltham, USA) diluted in 0.01% saponin/0.5%
495 BSA/PBS for 1 h at 37°C. The different parasite stages were detected through double-labelling
496 with stage-specific marker primary antibodies or 0.001% w/v Evans blue (Sigma Aldrich,

497 Taufkirchen, Germany) followed by incubation with Alexa Fluor 594-conjugated secondary
498 antibodies (Thermo Fisher Scientific (Waltham, USA) diluted in 0.01% saponin/0.5% BSA/PBS
499 for 1 h at 37°C. Nuclei were highlighted by treatment with Hoechst nuclear stain 33342 for 10
500 min at RT and cells were mounted with anti-fading solution AF2 (Citifluor Ltd) and sealed with
501 nail polish. Digital images were taken using a Leica AF 6000 microscope and processed using
502 Adobe Photoshop CS software.

503 **Asexual blood stage replication assay**

504
505 To compare the asexual blood stage replication between the parental WT and the ZNF4-KO
506 line, tightly synchronized ring stage cultures were set at an initial parasitemia of 0.25% and
507 the development of the parasite was followed by Giemsa-stained thin blood smears prepared
508 every 12 h over a time-period of 96 h at nine different time points (0, 12, 24, 36, 48, 60, 72,
509 84, 96 post-seeding). The parasitaemia of each time point was determined microscopically at
510 1,000-fold magnification by counting the percentage of parasites in 1,000 RBCs.

511 **Gametocyte development assay**

512
513 To determine the effect of ZNF4-KO on gametocyte development, WT and ZNF4-KO parasite
514 lines were tightly synchronized twice in two replication cycles and set to a parasitaemia of 5%
515 ring stage parasites. Gametocytogenesis was then induced by the addition of lysed RBCs
516 (0.5ml of 50 % haematocrit lysed RBC in 15ml of culture medium) followed by washing of the
517 cell the next day. The cultures were then maintained in cell culture medium supplemented
518 with 50 mM GlcNAc (N-acetyl glucosamine) to kill the asexual blood stages for 5 days [60] and
519 then maintained with normal cell culture medium till day 10 post induction. Samples were
520 taken in triplicate every 24 h starting from day 5 post induction for Giemsa smear preparation.
521 Gametocytaemia was determined per 1,000 RBCs and the gametocyte stages II-V at the

522 different time points from 50 gametocytes were counted in triplicate. For each assay, two
523 experiments were performed, each in triplicate.

524 **Exflagellation assay**

525
526 To determine the effect of *ZNF4* disruption on the ability of male gametocytes to exflagellate,
527 gametocytaemia of matured gametocytes of the WT and the *ZNF4*-KO parasite lines were
528 determined. 100 µl of each gametocyte culture was activated *in vitro* with 100 µM XA for 15
529 min at RT. After activation, the numbers of exflagellation centres were counted at 400-fold
530 magnification in 30 optical fields using a Leica DMLS microscope and the number of
531 exflagellation centres were adjusted with the gametocytaemia. Exflagellation was calculated
532 as a percentage of the number of exflagellation centres in the *ZNF4*-KO in relation to the
533 number of exflagellation centres in the WT control (WT set to 100%).

534 **Membrane feeding assay**

535
536 The effect of *ZNF4* depletion on malaria transmission was done by membrane feeding assays
537 performed at the TropIQ Health Science, Nijmegen Netherlands through the support of the
538 Infrastructure for the control of vector borne diseases (infravec2). Briefly, gametocyte
539 cultures of the WT and the *ZNF4*-KO lines were set up and on day 16, when the gametocytes
540 were fully matured, they were fed to female *Anopheles stephensi* mosquitoes using standard
541 membrane feeding assays. After 7 days the midguts were dissected and the oocysts were
542 counted following staining with mercurochrome.

543 **Statistical and online Analysis**

544
545 Statistical analysis of significant differences in exflagellation between WT and *ZNF4*-KO was
546 done using t-test with the help of the Graph Pad Prism software. *ZNF4* domain structure and
547 3D structure was predicted using UniProt (<https://www.uniprot.org/uniprot/Q8II18>) and

548 AlphaFold [25,26] respectively. Gene ontology (GO) enrichment analyses were determined
549 using PlasmoDB (plasmodb.org/plasmo/app). For GO analysis, the default settings were used
550 with $p < 0.05$. To compare transcript expression of top 30 down-regulated genes, a heat map
551 was constructed using TB tools [30].
552 To determine the enriched motifs in the de-regulated genes, the comprehensive motif analysis
553 tool XSTREME was used (meme-suite.org,[31]). Top 2 enriched motifs between 7 to 15
554 nucleotides in the de-regulated genes as compared to controls (48 genes with fold change
555 1.00) were considered. Transcripts of de-regulated genes as well as control were downloaded
556 from the PlasmoDB (plasmodb.org/plasmo/app).

557 Acknowledgements

558
559 We thank Fabian Bick for his assistance in ZNF4 protein expression and purification.

560 Author Contributions

561
562 Conceptualization: CJN and GP, Funding acquisition: CJN, GP and AF, Investigation: CJN, GP,
563 BH and AF, Methodology: CJN, BH, AF, Supervision: CJN, GP, writing -original draft: CJN,
564 Writing, review and editing: CJN, GP and AF.

565 Figure Legends

566

567 Fig 1: Domain architecture and protein expression of ZNF4.

568 (A) Schematic of the ZNF4 domain structure. The 204 kDa protein contains three CCCH zinc
569 finger domains indicated in red. The black line indicates the region used for the generation of
570 the recombinant peptide. (B) Predicted 3D structure of ZNF4. The 3D structure of the protein
571 was predicted using AlphaFold [25,26]. Colours indicate the confidence level of prediction
572 which ranged from blue (very high confidence) to orange (very low confidence). (C) Transcript
573 expression of ZNF4 in the blood stages of *P. falciparum*. Complementary DNA was synthesized
574 from rings (R), trophozoites (TZ), schizonts (SZ), immature (imGC), mature (mGC) and
575 gametocytes at 30 min post-activation (aGC) and subjected to diagnostic PCR using ZNF4-
576 specific primers. The expression levels of Pfama1 and Pfccp2 were used to verify asexual
577 blood stage and gamete-specific expression. Samples lacking reverse transcriptase (-RT)
578 were used as controls to check for any contamination with genomic DNA. Pffbp1a was used as

579 a loading control. (D) Localization of ZNF4 in different blood stages of *P. falciparum*. Anti-ZNF4
580 was used to immunolabel fixed samples of trophozoites, schizonts and gametocytes (GC stage
581 II to V) as well as of activated gametocytes (aGC) at 30 min post-activation (green). Asexual
582 blood stages (trophozoites and schizonts) were visualized by labelling with Evans blue and
583 gametocytes were visualized by using rabbit anti-Pfs230 (red); nuclei were highlighted by
584 Hoechst nuclear stain 33342 (blue). Bar, 5 μ m.
585

586 **Fig 2: Targeted gene disruption of ZNF4 and its effect on asexual blood stage replication and**
587 **gametocytogenesis.**

588 (A) Schematic depicting the generation of ZNF4-KO via single crossover recombination-based
589 gene disruption using selective linked integration targeted gene disruption (SLI-TGD). The
590 vector pSLI-TGD was modified to contain a 601 bp sequence block (white box with red stripes)
591 from near the 5' end of the ZNF4 coding region (red box). The coding region was maintained
592 in frame with a GFP protein coding region (green box), a 2A "skip" peptide (black box) and the
593 Neo-R gene (grey) that provides resistance to the antibiotic G418. Arrows indicate the position
594 of primers 1-4 used to detect integration of the pSLI-TGD vector. Asterisks indicate a stop
595 codon. GFP, green fluorescent protein; hDHFR; human dehydrofolate reductase for resistance
596 to WR99210; NeoR, neomycin-resistance; 2A, Skip peptide. (B) Confirmation of vector
597 integration for the ZNF4-KO parasites by diagnostic PCR using gDNA obtained from ZNF4-KO
598 and WT-NF54. 5'-integration was detected using primers 1 and 4 (1164 bp) and 3'-integration
599 using primers 3 and 2 (955 bp). Primers 3 and 4 were used to detect the presence of episome
600 (965 bp), and primers 1 and 2 were used for WT control (1194 bp). (C) Confirmation of
601 truncated ZNF4 tagged with GFP. Parasite lysates obtained from different stages of the ZNF4-
602 KO parasite line were subjected to Western blotting using polyclonal mouse anti-GFP
603 (estimated size 53 kDa). Lysate from WT mature gametocyte was used as negative control.
604 Immunoblotting with mouse anti-Pf39 antisera (39 kDa) served as a loading control. (D)
605 Verification of GFP expression in the ZNF4-KO parasites by live imaging. Live images of
606 trophozoites (TZ) and gametocyte stage II (GCII) of the ZNF4-KO line detected GFP (green) in
607 the parasite. Nuclei were counterstained with Hoechst 33342 (blue). Bar, 5 μ m. (E) Asexual
608 blood stage replication of the ZNF4-KO. Synchronized ring stage cultures of WT and ZNF4-KO
609 with an initial parasitaemia of 0.25% were maintained in cell culture medium and the
610 parasitaemia was followed over a time-period of 0 to 94 h via Giemsa stained smears. The
611 data is a representation of one of two experiments performed in triplicate (mean \pm SD). For
612 the second experiment see Fig S2A. (F) Disruption of ZNF4 show no effect in gametocytogenesis.
613 Following two rounds of synchronization, a culture 5% ring stage parasites of the WT and
614 ZNF4-KO was induced for gametocytogenesis and the next day the parasites were washed and
615 grown with medium supplemented with 50 mM GlcNac to kill asexual blood stages for 5 day,
616 then with normal medium till day 10 post induction. The gametocyte gametocytogenesis was
617 monitored by Giemsa stained blood smears from day 5 post induction. The result is a
618 representative of one of two experiments (see Fig S2B for second experiment). (H).
619 Gametocyte maturation in the ZNF4-KO. The development of gametocyte was compared
620 between the WT and the ZNF4-KO by counting the gametocyte stages of 50 gametocytes at
621 each time point in triplicate (See Fig 2C for second experiment). (H) Gametocyte morphology
622 in the ZNF4-KO line. Giemsa stained pictures of gametocyte stages of the ZNF4-KO and WT.
623

624 **Fig 3: ZNF4-KO impairs male gametocyte exflagellation and parasite transmission in the**
625 **mosquito** (A) Disruption of ZNF4 impairs male gametocyte exflagellation. Mature WT and
626 ZNF4-KO gametocytes were activated *in vitro* and the number of exflagellation centres

627 counted in 30 fields in triplicated using the light microscope. Three independent experiments
628 were performed indicated in numbers 1 to 3. **, $P < 0.05$, Student's t test. (B) Mosquito
629 infectivity of ZNF4-KO. Enriched mature gametocytes of WT or the ZNF4-KO were fed
630 to *An. stephensi* mosquitoes via standard membrane feeding assays. The numbers of oocysts
631 per midgut were counted at day 10 post infection in four independent experiments each.
632

633 **Fig 4: De-regulation of gene expression following disruption of ZNF4.**

634 (A) Comparative transcriptomics of de-regulated genes in the ZNF4-KO parasite line in rings
635 and mature gametocytes. Total RNA was extracted from ring stage parasites as well as mature
636 gametocytes of the ZNF4-KO and the WT and subjected to comparative transcriptomics by
637 RNA sequencing. De-regulated genes with relative gene expression greater than 2-fold was
638 considered significant. (B) Validation of RNA-Seq data by qRT. Transcript analysis for 5 up-
639 regulated genes and 3 down-regulated in mature gametocyte as identified by RNA-Seq were
640 validated by real-time RT-PCR. Transcript expression levels were calculated by the $2^{-\Delta Ct}$
641 method; the threshold cycle number (Ct) was normalized with the Ct of the gene encoding
642 seryl tRNA-ligase (PF3D7_0717700) as reference. Genes were considered up-regulated when
643 the changes between ZNF4-KO and WT sample were greater than 2-fold. (C, D) Summary of
644 Gene Ontology functional analysis of mature gametocyte differentially expressed genes
645 following ZNF4 disruption. GO enrichment analysis of de-regulated genes was determined
646 using PlasmoDB (<https://plasmodb.org/plasmo/app>). The most significantly ($P < 0.05$)
647 enriched GO terms in biological process, cellular component and molecular function are
648 presented. For the complete list see Table S1. All adjusted statistically significant values of the
649 terms were the absolute \log_{10} values. GO, gene ontology. (E) Pie chart showing peak
650 expression stage of de-regulated genes. The peak expression of the down-regulated as well as
651 up-regulated genes were determined using the 7 stage RNA-Seq data [28]. (F) Heat map of top
652 30 down-regulated genes and their sex-specific expression. Heat map representing patterns
653 of the top 30 down- regulated genes and their sex specific expression pattern [29]. Heat map
654 was constructed using TB tools [30].

655 **References**

1. WHO. World malaria report 2021. [cited 13 Jan 2022]. Available: <https://www.who.int/publications/i/item/9789240040496>
2. Bennink S, Kiesow MJ, Pradel G. The development of malaria parasites in the mosquito midgut. *Cell Microbiol.* 2016;18: 905–18. doi:10.1111/cmi.12604
3. Kuehn A, Pradel G. The coming-out of malaria gametocytes. *J Biomed Biotechnol.* 2010;2010: 976827. doi:10.1155/2010/976827
4. Josling GA, Llinás M. Sexual development in *Plasmodium* parasites: knowing when it's time to commit. *Nat Rev Microbiol.* 2015;13: 573–587. doi:10.1038/nrmicro3519
5. Kafsack BFC, Rovira-Graells N, Clark TG, Bancells C, Crowley VM, Campino SG, et al. A transcriptional switch underlies commitment to sexual development in malaria parasites. *Nature.* 2014;507: 248–52. doi:10.1038/nature12920
6. Sinha A, Hughes KR, Modrzynska KK, Otto TD, Pfander C, Dickens NJ, et al. A cascade of DNA-binding proteins for sexual commitment and development in *Plasmodium*. *Nature.* 2014;507: 253–7. doi:10.1038/nature12970
7. Shang X, Shen S, Tang J, He X, Zhao Y, Wang C, et al. A cascade of transcriptional repression determines sexual commitment and development in *Plasmodium falciparum*. *Nucleic Acids Res.* 2021;49: 9264. doi:10.1093/NAR/GKAB683

673 8. Yuda M, Kaneko I, Iwanaga S, Murata Y, Kato T. Female-specific gene regulation in
674 malaria parasites by an AP2-family transcription factor. *Mol Microbiol*. 2020;113: 40–
675 51. doi:10.1111/MMI.14334

676 9. Li Z, Cui H, Guan J, Liu C, Yang Z, Yuan J. Plasmodium transcription repressor AP2-O3
677 regulates sex-specific identity of gene expression in female gametocytes. *EMBO Rep*.
678 2021;22. doi:10.15252/EMBR.202051660

679 10. Kaneko I, Iwanaga S, Kato T, Kobayashi I, Yuda M. Genome-Wide Identification of the
680 Target Genes of AP2-O, a Plasmodium AP2-Family Transcription Factor. *PLOS Pathog*.
681 2015;11: e1004905. doi:10.1371/JOURNAL.PPAT.1004905

682 11. Modrzynska K, Pfander C, Chappell L, Yu L, Suarez C, Dundas K, et al. A Knockout
683 Screen of ApiAP2 Genes Reveals Networks of Interacting Transcriptional Regulators
684 Controlling the Plasmodium Life Cycle. *Cell Host Microbe*. 2017;21: 11–22.
685 doi:10.1016/J.CHOM.2016.12.003

686 12. Bennink S, Pradel G. The molecular machinery of translational control in malaria
687 parasites. *Mol Microbiol*. 2019;112: 1658–1673. doi:10.1111/mmi.14388

688 13. Bennink S, von Bohl A, Ngwa CJ, Henschel L, Kuehn A, Pilch N, et al. A seven-helix
689 protein constitutes stress granules crucial for regulating translation during human-to-
690 mosquito transmission of *Plasmodium falciparum*. *PLoS Pathog*. 2018;14.
691 doi:10.1371/journal.ppat.1007249

692 14. Mair GR, Lasonder E, Garver LS, Franke-Fayard BMD, Carret CK, Wiegant JCAG, et al.
693 Universal Features of Post-Transcriptional Gene Regulation Are Critical for
694 Plasmodium Zygote Development. *PLoS Pathog*. 2010;6: e1000767.
695 doi:10.1371/journal.ppat.1000767

696 15. Mair GR, Braks JAM, Garver LS, Wiegant JCAG, Hall N, Dirks RW, et al. Regulation of
697 sexual development of *Plasmodium* by translational repression. *Science*. 2006;313:
698 667–669. doi:10.1126/SCIENCE.1125129

699 16. Miao J, Li J, Fan Q, Li X, Li X, Cui L. The Puf-family RNA-binding protein PfPuf2 regulates
700 sexual development and sex differentiation in the malaria parasite *Plasmodium*
701 *falciparum*. *J Cell Sci*. 2010;123: 1039. doi:10.1242/JCS.059824

702 17. Shrestha S, Li X, Ning G, Miao J, Cui L. The RNA-binding protein Puf1 functions in the
703 maintenance of gametocytes in *Plasmodium falciparum*. *J Cell Sci*. 2016;129: 3144–
704 3152. doi:10.1242/JCS.186908

705 18. Ngwa CJ, Kiesow MJ, Papst O, Orchard LM, Filarsky M, Rosinski AN, et al.
706 Transcriptional Profiling Defines Histone Acetylation as a Regulator of Gene
707 Expression during Human-to-Mosquito Transmission of the Malaria Parasite
708 *Plasmodium falciparum*. *Front Cell Infect Microbiol*. 2017;7: 320.
709 doi:10.3389/fcimb.2017.00320

710 19. Ngwa CJ, Kiesow MJ, Orchard LM, Farrukh A, Llinás M, Pradel G. The g9a histone
711 methyltransferase inhibitor BIX-01294 modulates gene expression during plasmodium
712 *falciparum* gametocyte development and transmission. *Int J Mol Sci*. 2019;20.
713 doi:10.3390/ijms20205087

714 20. Ngwa CJ, Farrukh A, Pradel G. Zinc finger proteins of *Plasmodium falciparum*. *Cell*
715 *Microbiol*. 2021;23: e13387. doi:10.1111/CMI.13387

716 21. Hajikhezri Z, Darweesh M, Akusjärvi G, Punga T. Role of CCCH-Type Zinc Finger
717 Proteins in Human Adenovirus Infections. *Viruses*. 2020;12: 1–13.
718 doi:10.3390/v12111322

719 22. Taylor GA, Thompson MJ, Lai WS, Blackshear PJ. Mitogens stimulate the rapid nuclear
720 to cytosolic translocation of tristetraprolin, a potential zinc-finger transcription factor.

721 23. Mol Endocrinol. 1996;10: 140–146. doi:10.1210/MEND.10.2.8825554

722 23. Pomeranz MC, Hah C, Lin PC, Kang SG, Finer JJ, Blackshear PJ, et al. The Arabidopsis
723 tandem zinc finger protein AtTZF1 traffics between the nucleus and cytoplasmic foci
724 and binds both DNA and RNA. Plant Physiol. 2010;152: 151–165.
725 doi:10.1104/PP.109.145656

726 24. Pomeranz M, Finer J, Jang JC. Putative molecular mechanisms underlying tandem
727 CCHC zinc finger protein mediated plant growth, stress, and gene expression
728 responses. Plant Signal Behav. 2011;6: 647–651. doi:10.4161/PSB.6.5.15105

729 25. Jumper J, Evans R, Pritzel A, Green T, Figurnov M, Ronneberger O, et al. Highly
730 accurate protein structure prediction with AlphaFold. Nature. 2021;596: 583.
731 doi:10.1038/s41586-021-03819-2

732 26. Varadi M, Anyango S, Deshpande M, Nair S, Natassia C, Yordanova G, et al. AlphaFold
733 Protein Structure Database: massively expanding the structural coverage of protein-
734 sequence space with high-accuracy models. Nucleic Acids Res. 2022;50: D439–D444.
735 doi:10.1093/NAR/GKAB1061

736 27. Birnbaum J, Flemming S, Reichard N, Soares AB, Mesén-Ramírez P, Jonscher E, et al. A
737 genetic system to study Plasmodium falciparum protein function. Nat Methods.
738 2017;14: 450–456. doi:10.1038/nmeth.4223

739 28. López-Barragán MJ, Lemieux J, Quiñones M, Williamson KC, Molina-Cruz A, Cui K, et
740 al. Directional gene expression and antisense transcripts in sexual and asexual stages
741 of Plasmodium falciparum. BMC Genomics. 2011;12: 587. doi:10.1186/1471-2164-12-
742 587

743 29. Lasonder E, Rijpma SR, van Schaijk BCL, Hoeijmakers WAM, Kensche PR, Gresnigt MS,
744 et al. Integrated transcriptomic and proteomic analyses of *P. falciparum* gametocytes:
745 molecular insight into sex-specific processes and translational repression. Nucleic
746 Acids Res. 2016;44: 6087–6101. doi:10.1093/nar/gkw536

747 30. Chen C, Chen H, Zhang Y, Thomas HR, Frank MH, He Y, et al. TBtools: An Integrative
748 Toolkit Developed for Interactive Analyses of Big Biological Data. Mol Plant. 2020;13:
749 1194–1202. doi:10.1016/J.MOLP.2020.06.009

750 31. Grant CE, Bailey TL. XSTREME: Comprehensive motif analysis of biological sequence
751 datasets. [cited 21 Jan 2022]. doi:10.1101/2021.09.02.458722

752 32. Ray D, Kazan H, Cook KB, Weirauch MT, Najafabadi HS, Li X, et al. A compendium of
753 RNA-binding motifs for decoding gene regulation. Nature. 2013;499: 172–177.
754 doi:10.1038/NATURE12311

755 33. Zhang M, Wang C, Otto TD, Oberstaller J, Liao X, Adapa SR, et al. Uncovering the
756 essential genome of the human malaria parasite *Plasmodium falciparum* by
757 saturation mutagenesis. Science. 2018;360. doi:10.1126/SCIENCE.AAP7847

758 34. Müller K, Silvie O, Mollenkopf HJ, Matuschewski K. Pleiotropic Roles for the
759 *Plasmodium berghei* RNA Binding Protein UIS12 in Transmission and Oocyst
760 Maturation. Front Cell Infect Microbiol. 2021;11: 1–16.
761 doi:10.3389/fcimb.2021.624945

762 35. Aprea I, Raidt J, Höben IM, Loges NT, Nöthe-Menchen T, Pennekamp P, et al. Defects
763 in the cytoplasmic assembly of axonemal dynein arms cause morphological
764 abnormalities and dysmotility in sperm cells leading to male infertility. PLoS genetics.
765 2021. doi:10.1371/journal.pgen.1009306

766 36. Lindemann CB, Lesich KA. Flagellar and ciliary beating: The proven and the possible. J
767 Cell Sci. 2010;123: 519–528. doi:10.1242/jcs.051326

768 37. Stone W, Sawa P, Lanke K, Rijpma S, Oriango R, Nyaurah M, et al. A Molecular Assay

769 to Quantify Male and Female *Plasmodium falciparum* Gametocytes: Results From 2
770 Randomized Controlled Trials Using Primaquine for Gametocyte Clearance. 2017;216:
771 457–67. doi:10.1093/infdis/jix237

772 38. Bradley J, Stone W, Da DF, Morlais I, Dicko A, Cohuet A, et al. Predicting the likelihood
773 and intensity of mosquito infection from sex specific *plasmodium falciparum*
774 gametocyte density. *Elife*. 2018;7. doi:10.7554/ELIFE.34463

775 39. Leslie JS, Rawlins LE, Chioza BA, Olubodun OR, Salter CG, Fasham J, et al. MNS1 variant
776 associated with situs inversus and male infertility. *Eur J Hum Genet*. 2020;28: 50–55.
777 doi:10.1038/s41431-019-0489-z

778 40. Ta-Shma A, Hjeij R, Perles Z, Dougherty GW, Abu Zahira I, Letteboer SJF, et al.
779 Homozygous loss-of-function mutations in MNS1 cause laterality defects and likely
780 male infertility. *PLoS Genet*. 2018;14. doi:10.1371/JOURNAL.PGEN.1007602

781 41. Parkhurst SM, Meneely PM. Sex determination and dosage compensation: lessons
782 from flies and worms. *Science*. 1994;264: 924–932. doi:10.1126/SCIENCE.8178152

783 42. Wang J, Bell LR. The sex-lethal amino terminus mediates cooperative interactions in
784 RNA binding and is essential for splicing regulation. *Genes Dev*. 1994;8: 2072–2085.
785 doi:10.1101/gad.8.17.2072

786 43. Schmid M, Olszewski P, Pelechano V, Gupta I, Steinmetz LM, Jensen TH. The Nuclear
787 PolyA-Binding Protein Nab2p Is Essential for mRNA Production. *Cell Rep*. 2015;12:
788 128–139. doi:10.1016/J.CELREP.2015.06.008

789 44. Green DM, Marfatia KA, Crafton EB, Zhang X, Cheng X, Corbett AH. Nab2p is required
790 for poly(A) RNA export in *Saccharomyces cerevisiae* and is regulated by arginine
791 methylation via Hmt1p. *J Biol Chem*. 2002;277: 7752–7760.
792 doi:10.1074/JBC.M110053200

793 45. Kini HK, Kong J, Liebhaber SA. Cytoplasmic poly(A) binding protein C4 serves a critical
794 role in erythroid differentiation. *Mol Cell Biol*. 2014;34: 1300–1309.
795 doi:10.1128/MCB.01683-13

796 46. Miao J, Fan Q, Parker D, Li X, Li J, Cui L. Puf mediates translation repression of
797 transmission-blocking vaccine candidates in malaria parasites. *PLoS Pathog*. 2013;9:
798 e1003268. doi:10.1371/journal.ppat.1003268

799 47. Hirai M, Maeta A, Mori T, Mita T. Pb103 Regulates Zygote/Ookinete Development in
800 *Plasmodium berghei* via Double Zinc Finger Domains. *Pathogens*. 2021;10: 1536.
801 doi:10.3390/pathogens10121536

802 48. Fu M, Blackshear PJ. RNA-binding proteins in immune regulation: a focus on CCCH zinc
803 finger proteins. *Nat Publ Gr*. 2016 [cited 14 Jan 2022]. doi:10.1038/nri.2016.129

804 49. Ngwa CJ, Scheuermayer M, Mair GR, Kern S, Brügl T, Wirth CC, et al. Changes in the
805 transcriptome of the malaria parasite *Plasmodium falciparum* during the initial phase
806 of transmission from the human to the mosquito. *BMC Genomics*. 2013;14: 256.
807 doi:10.1186/1471-2164-14-256

808 50. Ifediba T, Vanderberg JP. Complete in vitro maturation of *Plasmodium falciparum*
809 gametocytes. *Nature*. 1981;294: 364–6. Available:
810 <http://www.ncbi.nlm.nih.gov/pubmed/7031476>

811 51. Lambros C, Vanderberg JP. Synchronization of *Plasmodium falciparum* erythrocytic
812 stages in culture. *J Parasitol*. 1979;65: 418–20. Available:
813 <http://www.ncbi.nlm.nih.gov/pubmed/383936>

814 52. Wagle P, Nikolić M, Frommolt P. QuickNGS elevates Next-Generation Sequencing data
815 analysis to a new level of automation. *BMC Genomics*. 2015;16. doi:10.1186/S12864-
816 015-1695-X

817 53. Dobin A, Davis CA, Schlesinger F, Drenkow J, Zaleski C, Jha S, et al. STAR: ultrafast
818 universal RNA-seq aligner. *Bioinformatics*. 2013;29: 15–21.
819 doi:10.1093/BIOINFORMATICS/BTS635

820 54. Pertea M, Pertea GM, Antonescu CM, Chang TC, Mendell JT, Salzberg SL. StringTie
821 enables improved reconstruction of a transcriptome from RNA-seq reads. *Nat
822 Biotechnol* 2015 333. 2015;33: 290–295. doi:10.1038/nbt.3122

823 55. Liao Y, Smyth GK, Shi W. featureCounts: an efficient general purpose program for
824 assigning sequence reads to genomic features. *Bioinformatics*. 2014;30: 923–930.
825 doi:10.1093/BIOINFORMATICS/BTT656

826 56. Livak KJ, Schmittgen TD. Analysis of Relative Gene Expression Data Using Real-Time
827 Quantitative PCR and the 2- $\Delta\Delta CT$ Method. *Methods*. 2001;25: 402–408.
828 doi:10.1006/meth.2001.1262

829 57. Salanti A, Staalsoe T, Lavstsen T, Jensen ATR, Sowa MPK, Arnot DE, et al. Selective
830 upregulation of a single distinctly structured var gene in chondroitin sulphate A-
831 adhering *Plasmodium falciparum* involved in pregnancy-associated malaria. *Mol
832 Microbiol*. 2003;49: 179–191. doi:10.1046/j.1365-2958.2003.03570.x

833 58. Wang CW, Mwakalinga SB, Sutherland CJ, Schwank S, Sharp S, Hermsen CC, et al.
834 Identification of a major rif transcript common to gametocytes and sporozoites of
835 *Plasmodium falciparum*. *Malar J*. 2010;9: 147. doi:10.1186/1475-2875-9-147

836 59. Kariuki MM, Kiaira JK, Mulaa FK, Mwangi JK, Wasunna MK, Martin SK. *Plasmodium
837 falciparum*: Purification of the various gametocyte developmental stages from in
838 vitro-cultivated parasites. *Am J Trop Med Hyg*. 1998;59: 505–508.

839 60. Fivelman QL, McRobert L, Sharp S, Taylor CJ, Saeed M, Swales CA, et al. Improved
840 synchronous production of *Plasmodium falciparum* gametocytes in vitro. *Mol
841 Biochem Parasitol*. 2007;154: 119–123. doi:10.1016/j.molbiopara.2007.04.008

842

843 Supporting Information captions

844

845 **Fig S1: Validation of ZNF4 protein expression using the pSLI-ZNF4-HA-glmS parasite line.** (A) Schematic depicting the single cross over homologous recombination strategy for the generation of the ZNF4-HA-glmS parasite line using the pSLI-HA-glmS vector and primer combinations for checking successful integration. (B) Diagnostic PCR to confirm vector integration using the ZNF4-HA-glmS parasite line. 5'-integration was detected using primers 5 and 8 (1543 bp) and 3'-integration using primers 7 and 6 (1253 bp). Primers 7 and 8 were used to detect the presence of episome (1348 bp), and primers 5 and 6 were used for WT control (1448 bp). (C) Confirmation of ZNF4 tagging with HA by Western blotting. Parasite lysates obtained from gametocytes of the ZNF4-HA-glmS parasite line were subjected to Western blotting using rat anti-HA. Lysates from non-infected red blood cells (niRBC) and WT mature gametocyte (WT-GC) were used as negative control. Immunoblotting with mouse anti-Pf39 antisera (39 kDa) served as a loading control. (D) Expression of ZNF4 in different blood stages of *P. falciparum* using the ZNF4-HA-glmS. Anti-rabbit HA was used to immunolabel fixed samples of trophozoites, schizonts and gametocytes (green). Asexual blood stages (trophozoites and schizonts) were visualized by labelling with mouse anti- Pf39 and gametocytes were visualized by using mouse anti-Pfs230 (red); nuclei were highlighted by Hoechst nuclear stain 33342 (blue). Bar, 5 μ m.

846

847

848

849

850

851

852

853

854

855

856

857

858

859

860

861

862

863 **Fig S2: Phenotypic characterization for ZNF4-KO.** Second experiment for the Asexual
864 development (A), Gametocytaemia (B) and gametocyte development (C) of the ZNF4-KO as
865 compared to WT.

866

867 **Table S1: List of ZNF4-KO de-regulated genes in gametocytes and rings and complete GO-
868 Analysis.**

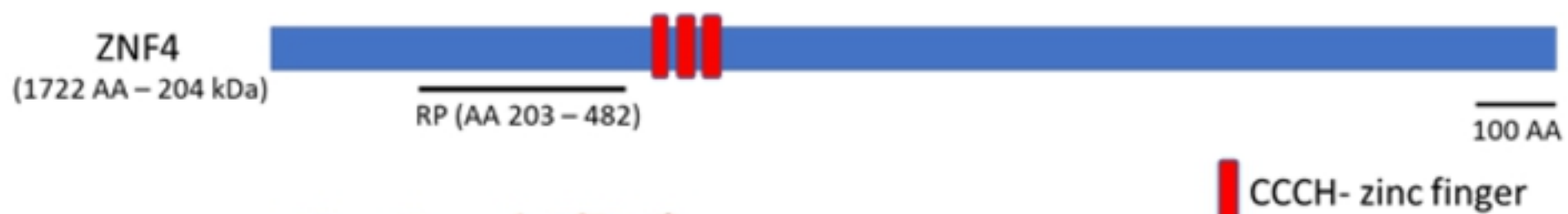
869

870 **Table S2: List of primers used in the study.**

871

872

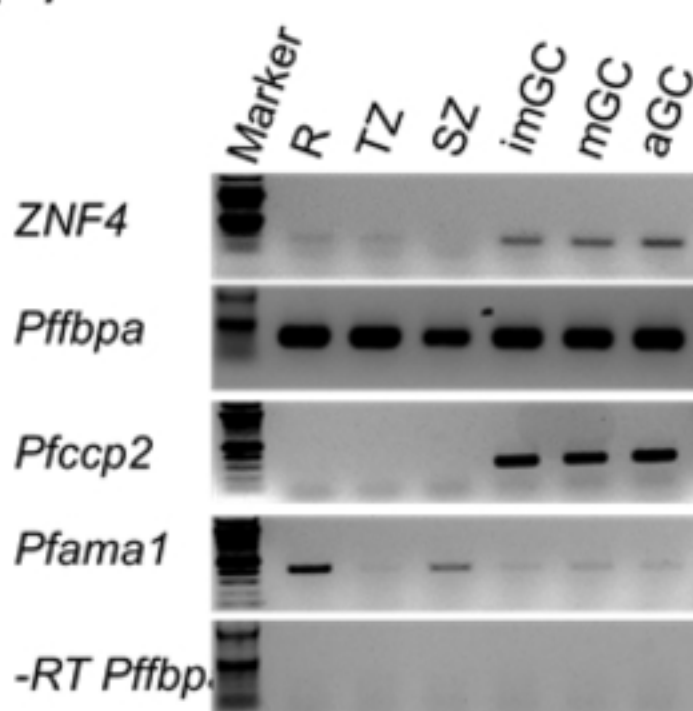
(A)



(B)

bioRxiv preprint doi: <https://doi.org/10.1101/2022.03.08.483571>; this version posted March 10, 2022. The copyright holder for this preprint (which was not certified by peer review) is the author/funder, who has granted bioRxiv a license to display the preprint in perpetuity. It is made available under aCC-BY 4.0 International license.

(C)



(D)

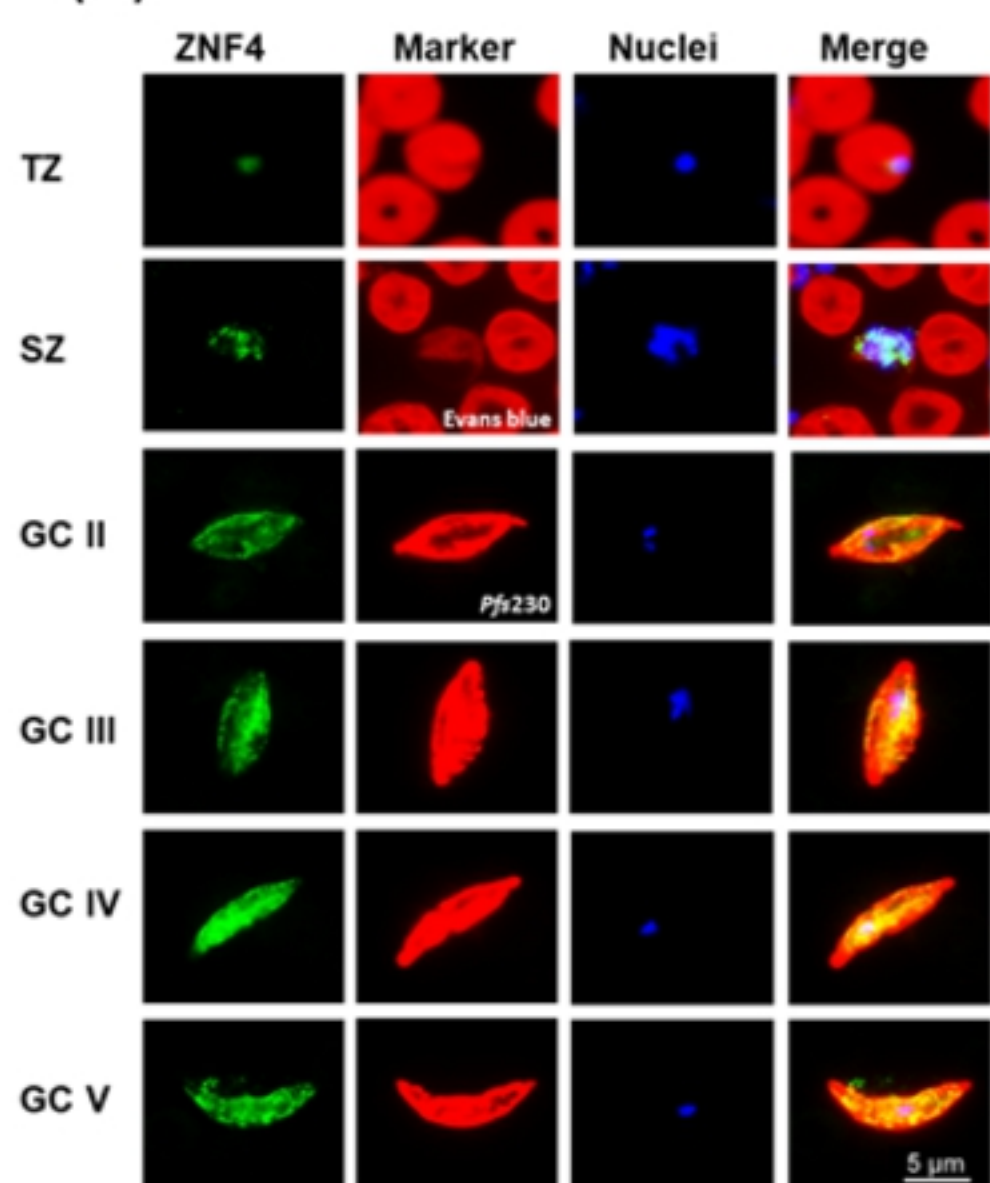


Fig 1

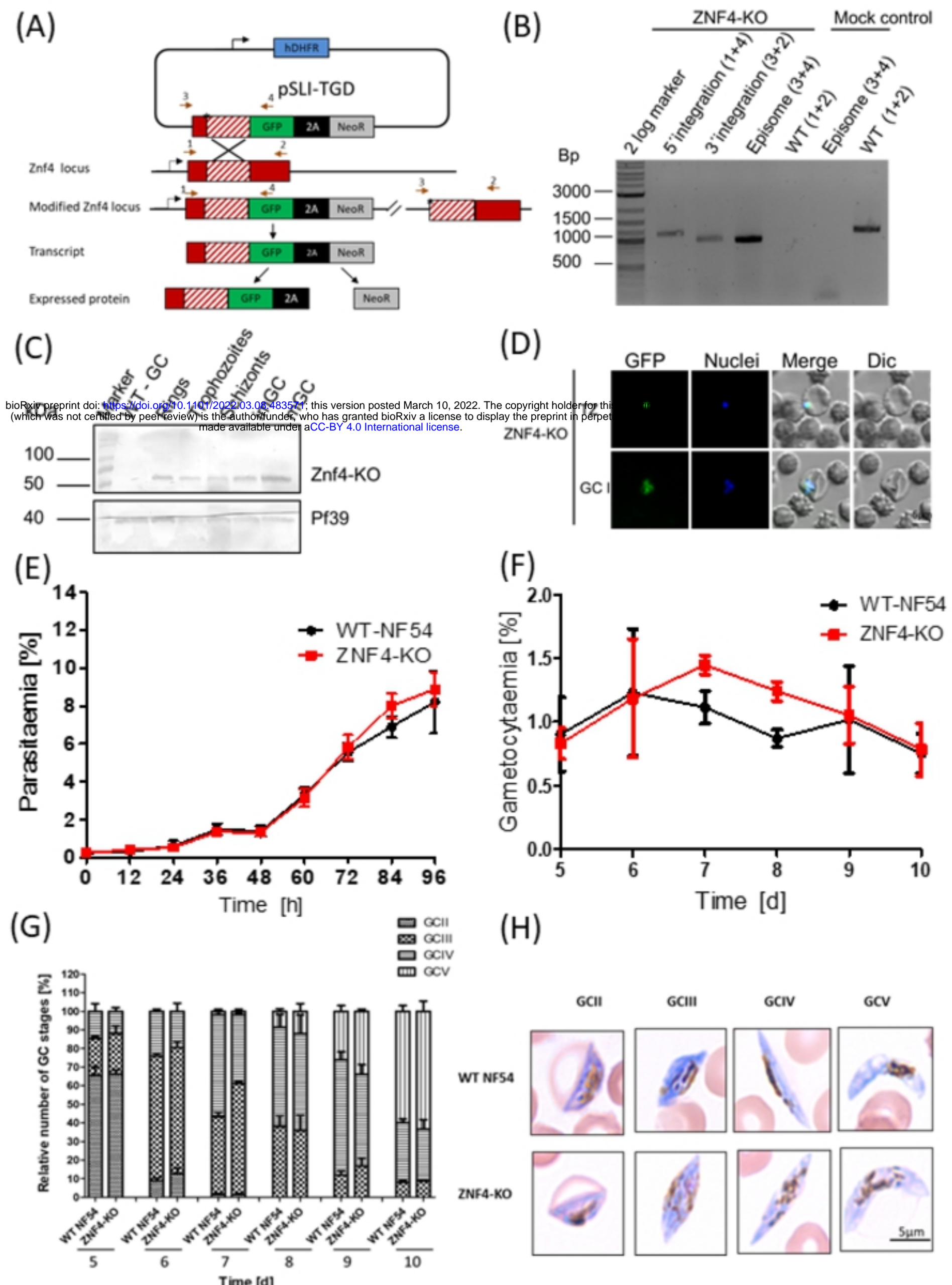
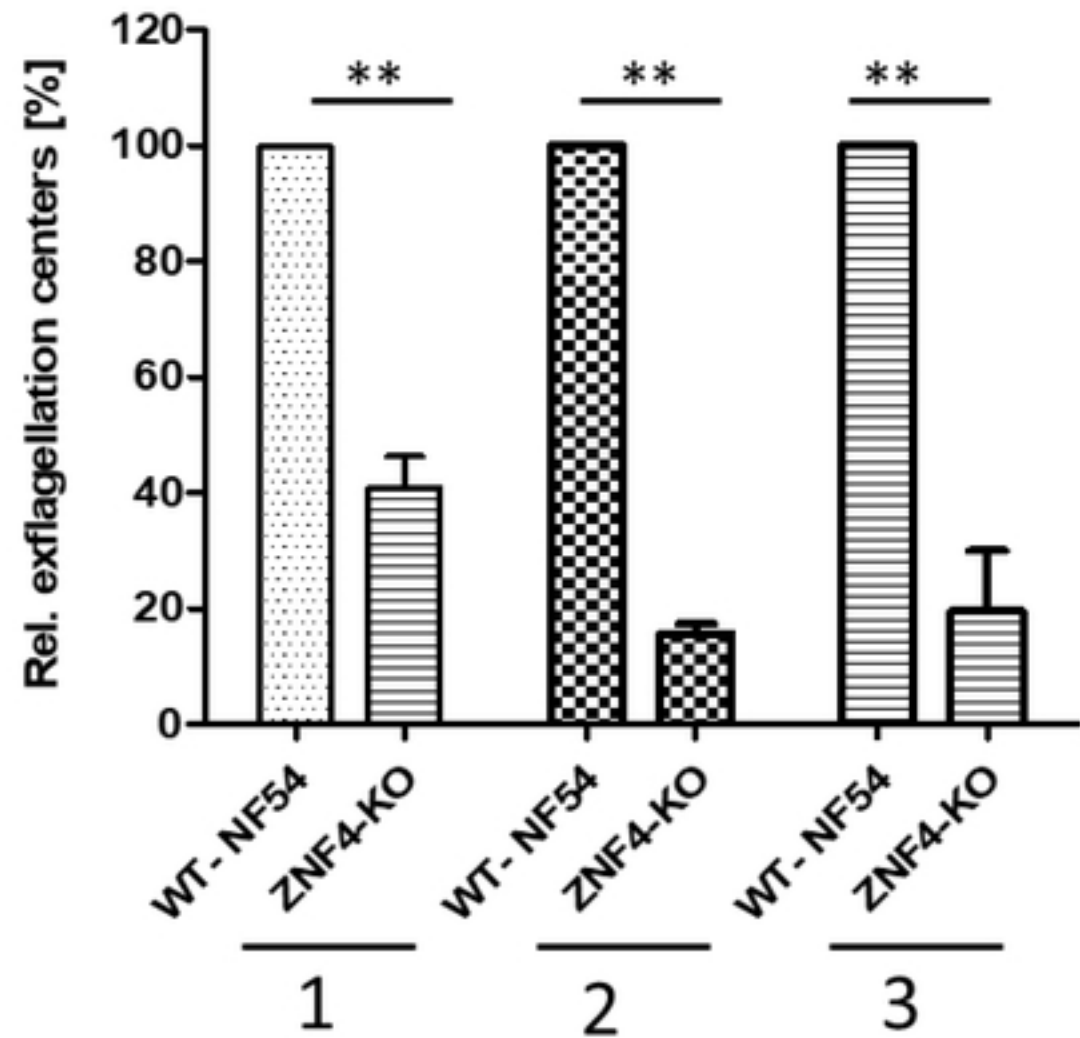


Fig 2

Figure 2

(A)



(B)

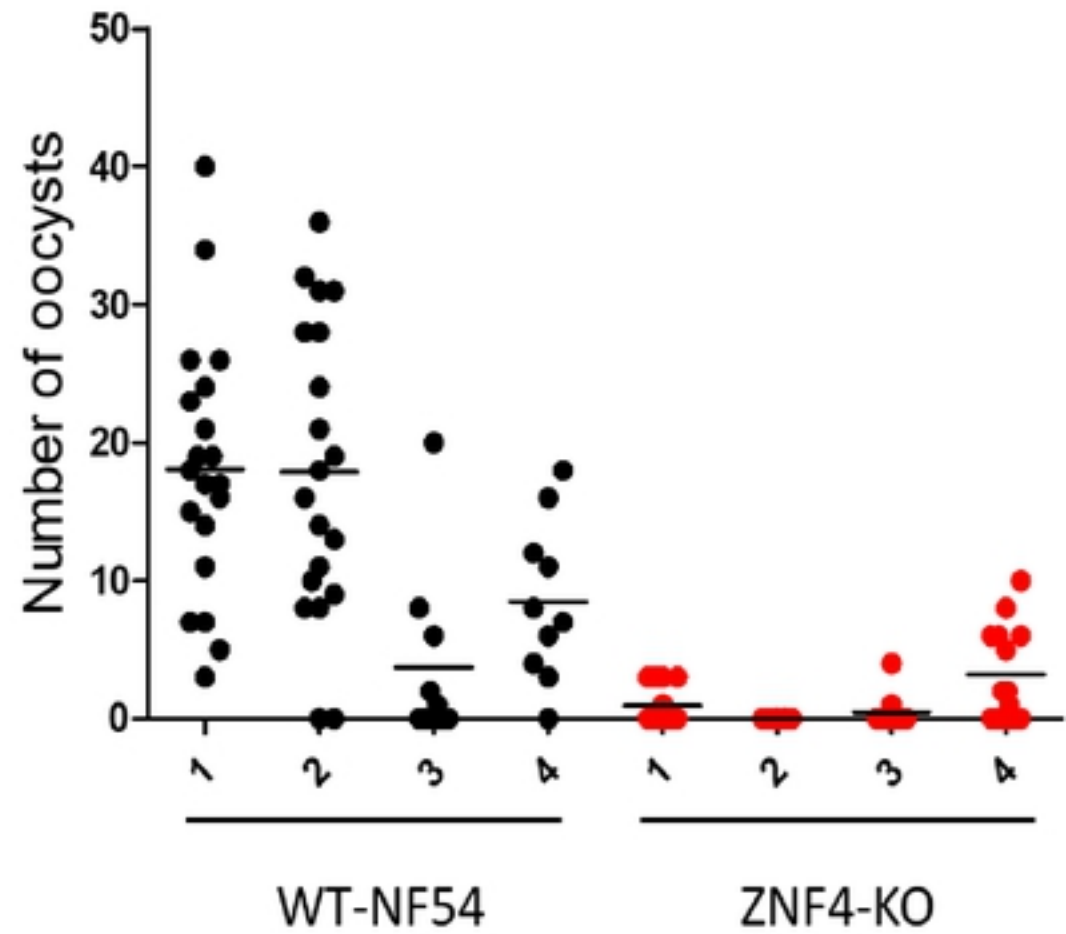
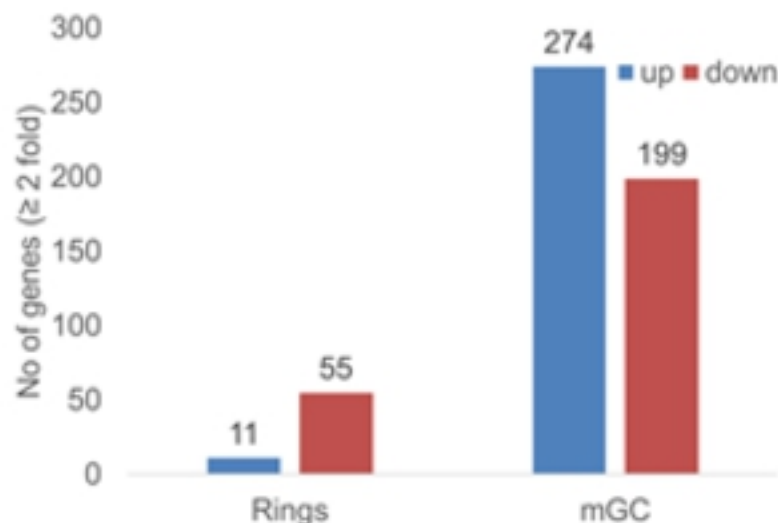


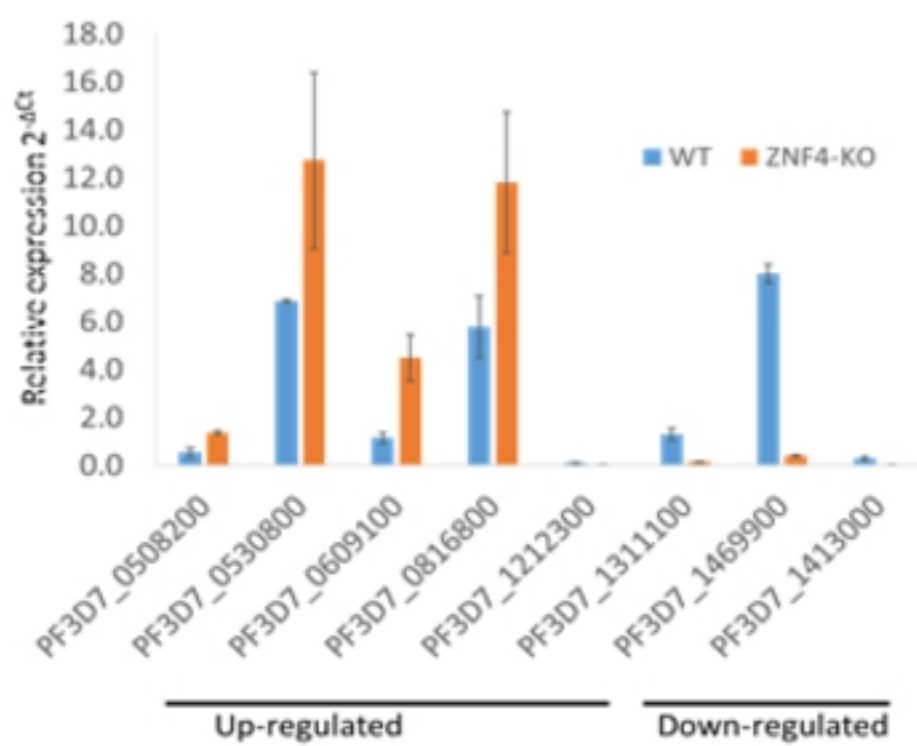
Fig 3

Figure 3

(A)

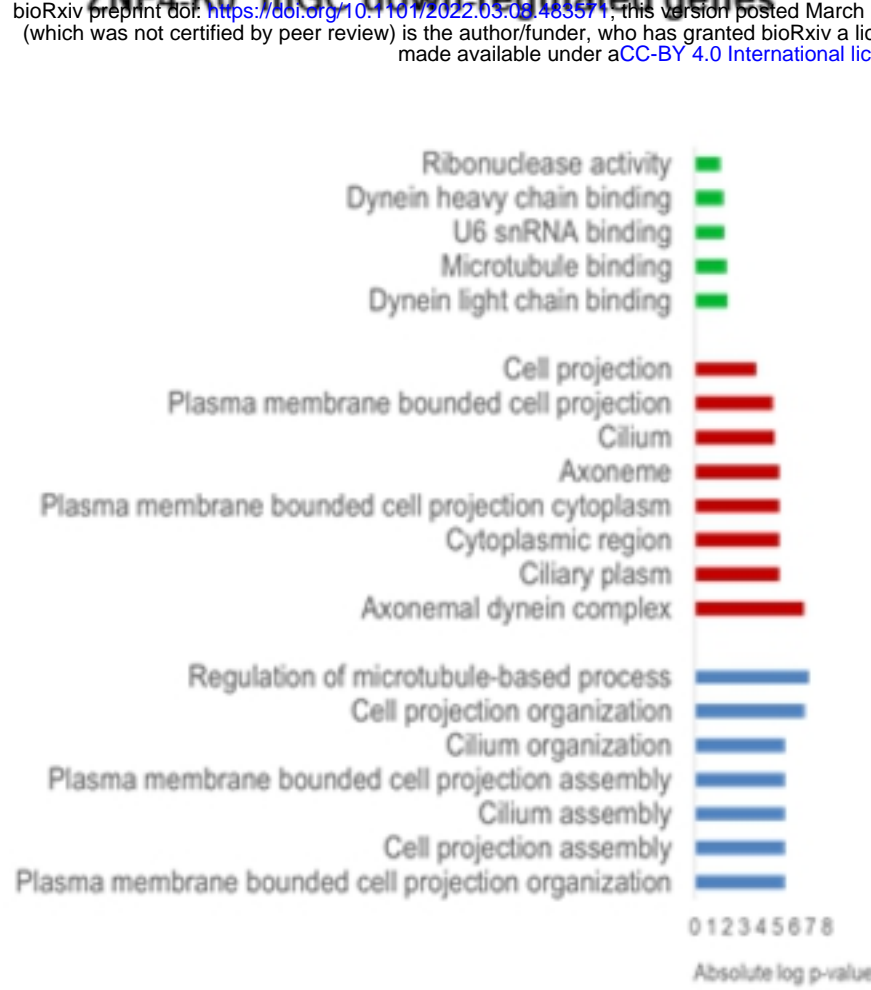


(B)



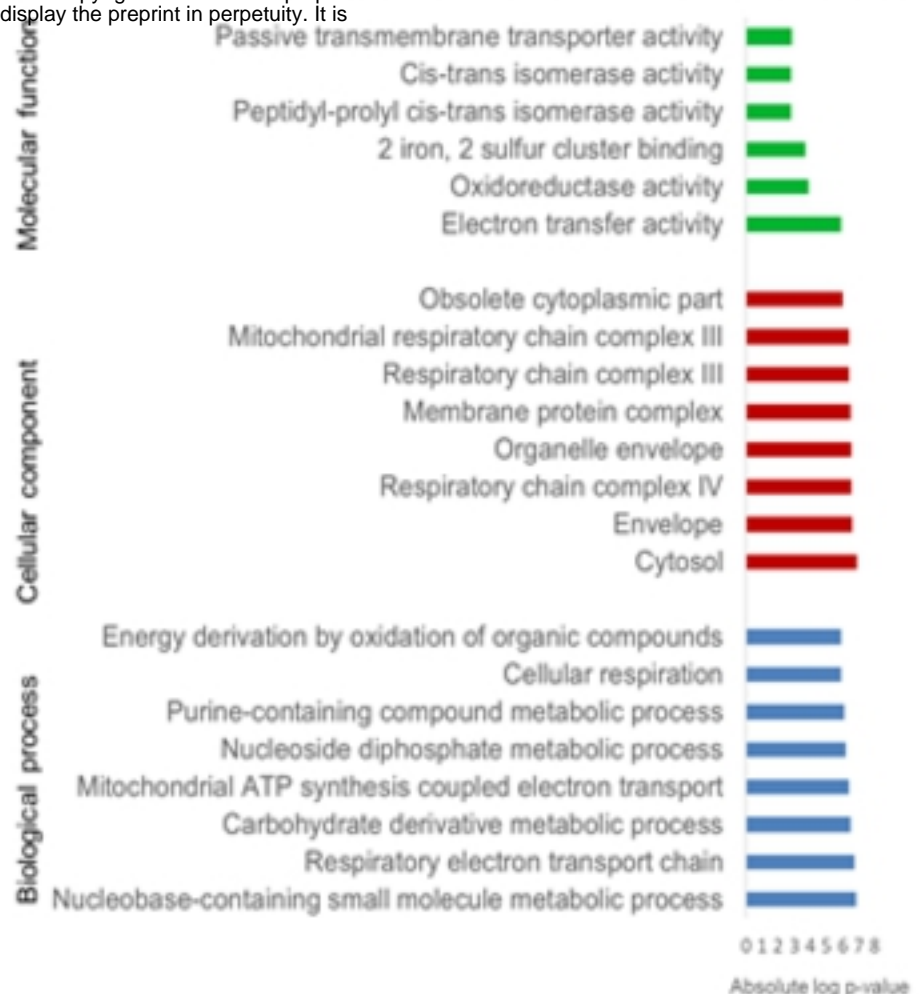
(C)

ZNF4-KO mGC down-regulated genes



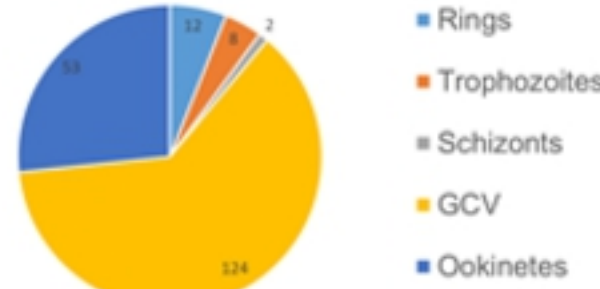
(D)

ZNF4-KO mGC up-regulated genes

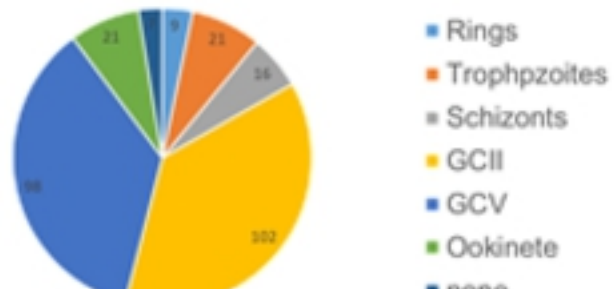


(E)

Peak expression of ZNF4-KO mGC down-regulated genes



Peak expression ZNF4-KO mGC up-regulated genes



(F)

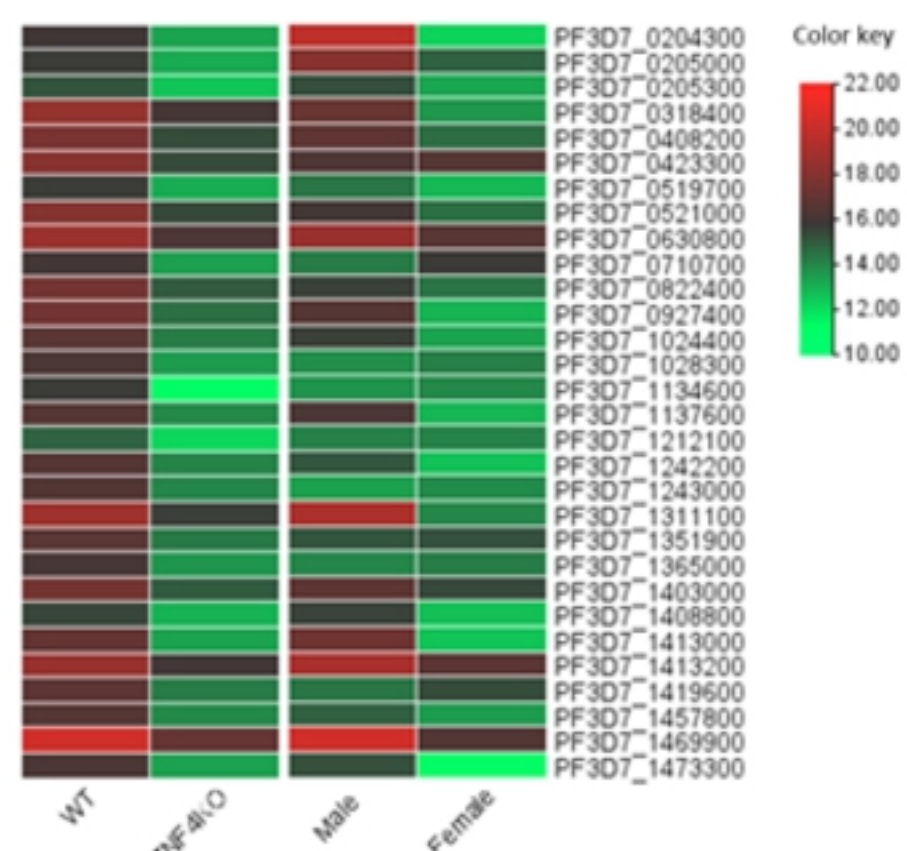


Fig 4

Figure 4